

# High-pressure spectroscopy studies on crystal fields and local structures of $\text{Pr}^{3+}$ in $\text{GdCl}_3$

ChunMao Li,<sup>1</sup> Kevin L. Bray,<sup>2</sup> and YongRong Shen<sup>2</sup>

<sup>1</sup>*Jiangsu Engineering Consulting Center, Nanjing 210003, People's Republic of China*

<sup>2</sup>*Department of Chemistry, Washington State University, Pullman, Washington 99164-4630*

(Received 29 September 2002; revised manuscript received 27 November 2002; published 6 March 2003)

The pressure dependence of 20-K luminescence and excitation spectra for  $\text{Pr}^{3+}$  ions in  $\text{GdCl}_3$  has been studied up to 60 kbar. The variations of the Slater parameters  $F_k$ , the spin-orbit coupling parameter  $\zeta_{4f}$ , and the crystal-field parameters  $B_q^k$  with pressure were evaluated from the observed crystal-field energy levels as a function of pressure. Based on the continuous variations of the crystal-field parameters with pressure, we focused on a discussion of the anomalous behavior in the  $^1D_2$  crystal-field splittings for  $\text{Pr}^{3+}$  in  $\text{GdCl}_3$  and the local structure of  $\text{Pr}^{3+}$  at  $\text{Gd}^{3+}$  in  $\text{GdCl}_3$ . The present results for  $\text{Pr}^{3+}:\text{GdCl}_3$  indicated that the anomalous  $^1D_2$  crystal-field splittings are described reasonably by an orbitally correlated crystal-field model. The local structure around substitutional  $\text{Pr}^{3+}$  ions in  $\text{GdCl}_3$  was discussed quantitatively within the superposition model.

DOI: 10.1103/PhysRevB.67.125106

PACS number(s): 78.55.Hx, 71.70.Ch, 62.50.+p

## I. INTRODUCTION

When a dopant ion is substitutionally incorporated into a crystal, a mismatch in ionic size results in local distortions around the dopant ion. The local distortions can be especially large when charge-compensating codopants are required to incorporate a dopant ion into a host lattice. The basic problem of understanding the structural distortions accompanying a dopant in substitution has stimulated much research, most of which has focused on the analysis of electron paramagnetic resonance spectra of paramagnetic dopant ions in host crystals.<sup>1-4</sup>

The well-known superposition model<sup>5,6</sup> provides a reasonable alternative approach for studying crystal-field (CF) and local distortion effects of lanthanide dopants, because it can relate local bond lengths and angles to spectroscopically determinable CF parameters ( $B_q^k$ ) of lanthanides. This model advantageously allows the  $B_q^k$  parameters to be separated into physical and geometric contributions according to

$$B_q^k = \sum_L \bar{B}_k(R_L) K_{kq}(\Theta_L, \Phi_L), \quad (1)$$

where the sum is over the nearest-neighboring ligands  $L$  located at the coordinates  $(R_L, \Theta_L, \Phi_L)$  relative to the dopant ion, and the geometric  $K_{kq}(\Theta_L, \Phi_L)$  coordination factors are known angular functions of the ligand ions. The parameters  $\bar{B}_k(R_L)$ , usually referred to as physical parts or intrinsic CF parameters, absorb all the physical contributions from the ligands and depend only on the ligand type and the interionic distance  $R_L$ . A power-law exponent is commonly used to express the distance dependence of the intrinsic CF parameters:  $\bar{B}_k(R) = \bar{B}_k(R_0)(R_0/R)^{t_k}$ , where  $R_0$  is an arbitrarily fixed reference distance.<sup>6</sup> For the special case of the electrostatic point-charge model,  $t_k$  is equal to  $k+1$ . Once the intrinsic CF parameters for a given lanthanide ion are determined in several host crystals based on a given type of coordinating ligands, it becomes possible to make reasonable predictions of CF interactions for the lanthanide ion in other host systems with the same type of coordinating ligands.

This means that the intrinsic CF parameters for a given ion-ligand pair arise from a similar physical origin, regardless of the host lattice, and that they are nearly transferable. Thus, the superposition model can be used to deduce the local structure (nearest-neighboring ligand positions) around lanthanide ions in host crystals, provided that  $B_q^k$  and  $\bar{B}_k(R)$  are obtained experimentally.

High pressure, which is a useful technique for gaining insight into CF interactions, can be used to obtain the intrinsic CF parameters  $\bar{B}_k(R_0)$  and their distance dependences  $t_k$ , because of its ability to continuously tune interionic distances. High-pressure spectroscopic and structural measurements of lanthanide ions in several host crystals have achieved the CF interaction strength as a function of distance.<sup>7-9</sup> An initial attempt was made within the superposition model to study the local distortions around  $\text{Sm}^{2+}$  in  $\text{CaFCl}$  using high-pressure luminescence spectroscopy.<sup>10</sup> Encouraging results were obtained and suggest that high-pressure investigations of local distortions of optically active impurity ions will be fruitful.

Although the considerable success of a conventional one-electron CF model has been achieved in rationalizing electronic structures of lanthanide ions in crystals, it is well known that certain lanthanide multiplets (e.g.,  $^1D_2$  of  $\text{Pr}^{3+}$ ,  $^2H_{11/2}$  of  $\text{Nd}^{3+}$ , and  $^5D_J$  of  $\text{Eu}^{3+}$ ) show anomalous CF splittings and are not reasonably described by the conventional one-electron CF model. An enormous amount of effort<sup>11-18</sup> indicated that such anomalous CF splittings occur in "standard" CF analyses due to the neglect of two-electron correlation crystal-field (CCF) effects. The largely increased number of new parameters has hindered the wide application of the CCF model to a practical lanthanide system that can only provide a limited number of experimental data.

In this paper, we consider the effect of pressure on the energy-level structure and local structure of  $\text{Pr}^{3+}$  in  $\text{GdCl}_3$ . We begin by measuring luminescence and excitation spectra of  $\text{Pr}^{3+}:\text{GdCl}_3$  as a function of pressure. Energies of 28 CF energy levels are determined up to 60 kbar and analyzed with conventional CF theory to obtain the  $B_q^k$  parameters as a function of pressure. We show that the conventional one-

electron CF theory is unable to account for  $^1D_2$  CF splittings of  $\text{Pr}^{3+}$  in  $\text{GdCl}_3$ . We propose a simple model, by analogy to previous studies<sup>19,20</sup> on  $^2H_{11/2}$  CF splittings of  $\text{Nd}^{3+}$  and  $^5D_J$  CF splittings of  $\text{Eu}^{3+}$  based on correction factors to the reduced matrix elements, to explain the  $^1D_2$  CF splitting of  $\text{Pr}^{3+}$ . We also use the superposition model to determine the local structure of substitutional  $\text{Pr}^{3+}$  ions in the  $\text{GdCl}_3$  lattice.

## II. EXPERIMENT AND RESULTS

Single crystals of  $\text{GdCl}_3$  grown by the standard Bridgman technique contained a concentration of 1 mol %  $\text{Pr}^{3+}$ . High pressure was generated by a gasketed diamond-anvil cell (DAC) and spectroscopic oil (polychlorotrifluoroethylene) as the pressure transmitting medium, and determined by the ruby  $R_1$ -line redshift. For low-temperature measurements, the DAC was mounted in a closed cycle refrigerator. The  $\text{Pr}^{3+}$  luminescence was dispersed by a double spectrometer and detected with a photomultiplier tube using the photon counting technique. An  $\text{Ar}^+$  laser and a dye laser were employed as excitation sources. In the present study, two  $\text{Ar}^+$  laser lines of 472.7 and 488.0 nm and tunable dye laser wavelengths from Rhodamine 6G were selected to directly excite the  $^3P_1$ ,  $^3P_0$ , and  $^1D_2$  levels, respectively, of  $\text{Pr}^{3+}$  in  $\text{GdCl}_3$ .

All high-pressure luminescence and excitation spectra of  $\text{Pr}^{3+}:\text{GdCl}_3$  were measured at  $\sim 20$  K. Sixteen groups of luminescence lines were observed over a spectral range from 11 500 to 21 000  $\text{cm}^{-1}$  and are assigned to  $^3P_{0,1} \rightarrow ^3H_{4-6}$ ,  $^3F_{2-4}$  and  $^1D_2 \rightarrow ^3H_{4-6}$ ,  $^3F_2$  transitions. Upon excitation to either the  $^3P_0$  or  $^3P_1$  levels, the luminescence from  $^1D_2$  was extremely weak. When the dye laser excitation source was used to directly excite the  $^1D_2$  multiplet, much stronger  $^1D_2 \rightarrow ^3H_{4-6}$  and  $^1D_2 \rightarrow ^3F_2$  luminescence transitions were observed. The dye laser wavelengths were adjusted at each pressure to compensate for pressure-induced changes in the energy of the  $^1D_2$  multiplet. The  $^3H_4 \rightarrow ^1D_2$  excitation spectrum under pressure was performed by monitoring the  $^1D_2(\Gamma_1) \rightarrow ^3H_6(\Gamma_4)$  luminescence line varying between 12 150 and 12 450  $\text{cm}^{-1}$  with pressure. Two representative  $^3H_4 \rightarrow ^1D_2$  excitation and  $^1D_2 \rightarrow ^3H_4$  luminescence spectra at 1 kbar and 38 kbar are shown in Fig. 1 with a schematic transition diagram. Since there is a very similar feature of the  $\text{Pr}^{3+}$  spectra in isostructural trichlorides such as  $\text{LaCl}_3$  (Refs. 7 and 8), all the observed luminescence and excitation lines were unambiguously assigned with the CF energy levels. Energies of most of CF energy levels were determined generally based on two and/or three different luminescence transitions. The energies of 28 measured CF energy levels for  $\text{Pr}^{3+}:\text{GdCl}_3$  as a function of pressure between ambient pressure and 60 kbar are summarized in Figs. 2(a–c).

## III. CALCULATION OF CF ENERGY LEVELS

Energy levels of lanthanide ions in solids are described by the free-ion ( $H_{\text{FI}}$ ) and CF Hamiltonian ( $H_{\text{CF}}$ ):

$$H = H_{\text{FI}} + H_{\text{CF}},$$

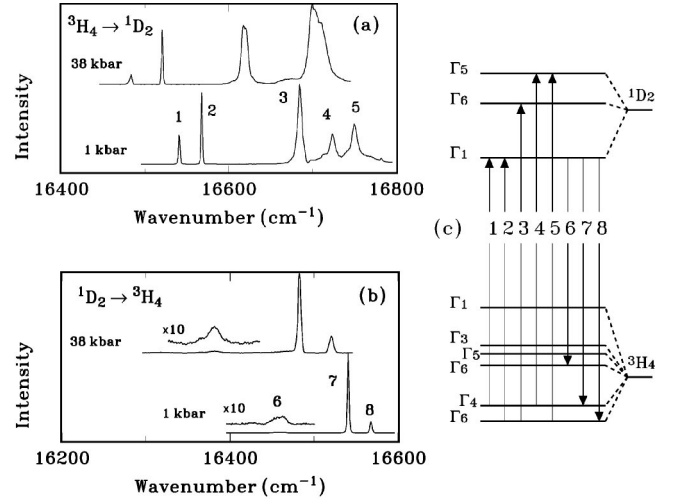


FIG. 1. (a) 20-K  $^3H_4 \rightarrow ^1D_2$  excitation spectra and (b)  $^1D_2 \rightarrow ^3H_4$  luminescence spectra of  $\text{Pr}^{3+}:\text{GdCl}_3$  at 1 and 38 kbar. (c) A schematic transition diagram.

where the free-ion Hamiltonian ( $H_{\text{FI}}$ ) primarily contains the Coulomb repulsion interaction and spin-orbit coupling. Higher-order interactions, such as the electrostatic and magnetically correlated configuration interactions,<sup>21</sup> are considered usually in a more accurate model description. The Coulomb interaction and spin-orbit coupling are parametrized with a set of Slater parameters  $F_k$  or  $F^k$  ( $k=2,4,6$ ) and one spin-orbit coupling parameter  $\zeta_{4f}$ . In the one-electron CF approximation, the CF Hamiltonian ( $H_{\text{CF}}$ ) is expressed by

$$H_{\text{CF}} = \sum_{kq} B_q^k C_q^{(k)},$$

where  $C_q^{(k)}$  are the spherical tensor operators and whose matrix elements can be calculated exactly. According to the requirement of a site symmetry, some CF parameters are left in  $H_{\text{CF}}$  and there are four nonzero CF parameters  $B_2^0, B_4^0, B_6^0$ , and  $B_6^6$  in the  $D_{3h}$  site symmetry that approximates to the site symmetry of  $\text{Pr}^{3+}$  at  $\text{Gd}^{3+}$  sites in  $\text{GdCl}_3$  (Ref. 22).

The experimental data shown in Figs. 2(a–c) were used to evaluate three  $F_k$ , one  $\zeta_{4f}$ , and four  $B_q^k$  parameters using a least-squares-fit method. In our fitting procedures, the higher-order interactions were also taken into account and the corresponding parameters ( $\alpha, \beta, \gamma, M^0, P^2$ ) were held fixed at their  $\text{Pr}^{3+}:\text{LaCl}_3$  values<sup>8</sup> for all calculations of our  $\text{Pr}^{3+}:\text{GdCl}_3$  system. For a comparison of our present results for  $\text{Pr}^{3+}:\text{GdCl}_3$  with previous results<sup>8</sup> for  $\text{Pr}^{3+}:\text{LaCl}_3$ , both ambient pressure values for the evaluated parameters are summarized in Table I.

Variations of these parameters with pressure were obtained using the same fitting approach. The standard deviation  $\sigma$  remained nearly constant ( $\sigma=8.8 \text{ cm}^{-1}$  at ambient pressure and  $\sigma=9.4 \text{ cm}^{-1}$  at 60 kbar). The  $F_k$  and  $\zeta_{4f}$  parameters showed a nearly linear reduction with pressure, which is ascribed to an increased nephelauxetic effect (for details, cf. Refs. 7 and 16). The relative decreases in  $F_2, F_4,$

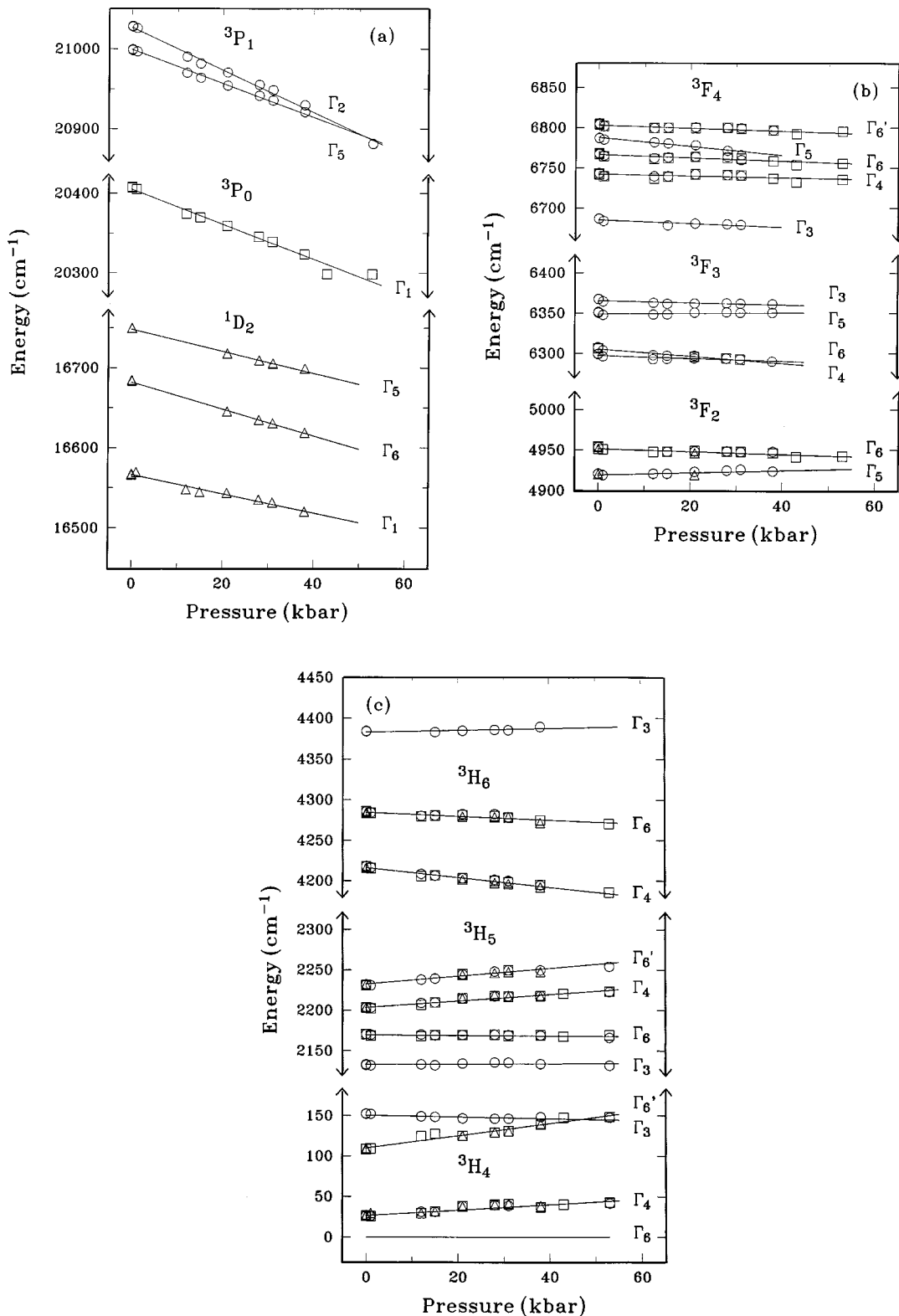


FIG. 2. (a)–(c) Energies of the CF energy levels as a function of pressure for  $\text{Pr}^{3+}:\text{GdCl}_3$ . Empty circles, squares, and triangles denote the identification results from the  $^3P_1$ ,  $^3P_0$ , and  $^1D_2$  transitions, respectively. The energies for all the CF energy levels are shown here with respect to the  $^3H_4(\Gamma_6)$  ground state.

$F_6$ , and  $\zeta_{4f}$  up to 60 kbar are  $-0.7(1)\%$ ,  $-0.6(1)\%$ ,  $-0.5(1)\%$ , and  $-0.3(1)\%$ , respectively. The reduction in the average Slater parameters  $F^k$  with pressure is twice as large as the spin-orbit coupling parameter  $\zeta_{4f}$  in our present

system and consistent with the previous observation<sup>8</sup> for  $\text{Pr}^{3+}$  in  $\text{LaCl}_3$  and  $\text{PrCl}_3$ , all of which are within the expectation of the central-field covalency mechanism describing the nephelauxetic effect.<sup>7,16</sup>

TABLE I. Parameters ( $\text{cm}^{-1}$ ) for  $\text{Pr}^{3+}$  in  $\text{GdCl}_3$  and  $\text{LaCl}_3$  at ambient pressure with statistical uncertainties given in parentheses. The number of CF energy levels included in the fits is given by  $N$ , and  $\sigma$  denotes the standard deviation ( $\text{cm}^{-1}$ ) between experimental and calculated energies of the energy levels. Values for the higher-order interaction parameters of  $\text{Pr}^{3+}:\text{GdCl}_3$  are held fixed at their  $\text{Pr}^{3+}:\text{LaCl}_3$  values ( $\alpha=22.81 \text{ cm}^{-1}$ ,  $\beta=-676 \text{ cm}^{-1}$ ,  $\gamma=1453 \text{ cm}^{-1}$ ,  $M^0=1.72 \text{ cm}^{-1}$ , and  $P^2=266 \text{ cm}^{-1}$ ).<sup>8</sup>

	$\text{Pr}^{3+}:\text{LaCl}_3$		$\text{Pr}^{3+}:\text{GdCl}_3$	
$F_2/F^2$	304.1(2)/68422(45)	298.5/67163	303.0(1)/68175(23)	302.9(1)/68153(23)
$F_4/F^4$	46.07(6)/50170(65)	43.92/47829	45.99(6)/50083(65)	45.96(9)/50050(98)
$F_6/F^6$	4.478(9)/32965(66)	4.104/30212	4.466(5)/32877(37)	4.467(9)/32884(66)
$\zeta_{4f}$	746(1)	753	746(1)	745(1)
$B_0^2$	118(7)	107	106(8)	102(18)
$B_0^4$	-334(12)	-459	-460(20)	-485(32)
$B_0^6$	-668(17)	-747	-741(29)	-724(43)
$B_6^6$	442(11)	480	477(19)	465(24)
$N$	29	45	45	28
$\sigma$	5.5	9.6	9.1	8.8
Ref.	8	23	This work	This work

The four CF parameters  $B_q^k$  of  $\text{Pr}^{3+}$  in  $\text{GdCl}_3$  varied linearly with pressure (Fig. 3). The  $B_0^6$  and  $B_6^6$  parameters showed strong increases in their absolute values with slopes of  $-2.28 \text{ cm}^{-1}/\text{kbar}$  and  $2.14 \text{ cm}^{-1}/\text{kbar}$ , respectively. The  $B_0^4$  and  $B_0^2$  parameters decreased in their absolute values at rates of  $0.90 \text{ cm}^{-1}/\text{kbar}$  and  $-1.54 \text{ cm}^{-1}/\text{kbar}$ , respectively.

#### IV. ANOMALOUS $^1D_2$ CRYSTAL-FIELD SPLITTINGS

As well known, CF splittings in the  $^1D_2$  multiplet of  $\text{Pr}^{3+}$  in many compounds are simulated poorly in comparison with the other multiplets in the framework of the conventional one-electron CF model.<sup>13</sup> In our present  $\text{Pr}^{3+}:\text{GdCl}_3$  system,

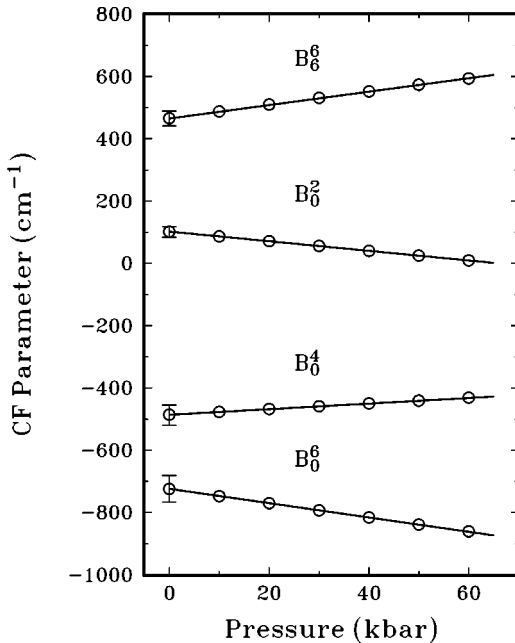


FIG. 3. Variations of the CF parameters  $B_q^k$  for  $\text{Pr}^{3+}:\text{GdCl}_3$  with pressure. Error bars given at ambient pressure represent the statistical errors only.

the  $^1D_2$  multiplet splits into three CF energy levels  $\Gamma_1$ ,  $\Gamma_5$ , and  $\Gamma_6$  and its discrepancy between the experimental and calculated energies just for its three energy levels is already responsible for 23% of the overall standard deviation  $\sigma$  at ambient pressure, and remained nearly constant up to 60 kbar (Fig. 4).

Like the  $^1D_2$  multiplet of  $\text{Pr}^{3+}$ , such as, for example, the  $^2H_{11/2}$  multiplet of  $\text{Nd}^{3+}$  or the  $^5D_{1,2}$  multiplets of  $\text{Eu}^{3+}$ , anomalous CF splittings that are persistent from host to host also hold. There is a great deal of interest in identifying how the conventional CF model may be improved to deal with these anomalous multiplets. There are two major theoretical strategies. The first one is to extend the one-electron CF model to a two-electron CCF model.<sup>24</sup> The second is to consider interactions between the ground configuration ( $4f^N$ ) and excited configurations ( $4f^{N-1}nl$ ) of lanthanide ions and to extend the set of basis wave functions in CF calculations.<sup>12,25</sup> Unfortunately, both strategies are impracticable in the CF calculations because a large number of new

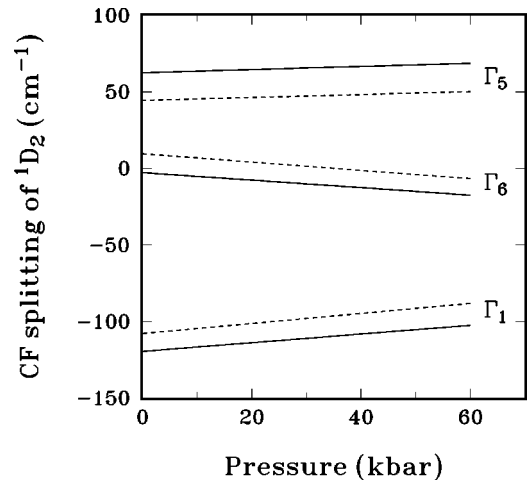


FIG. 4. Variations of the  $^1D_2$  CF splittings for  $\text{Pr}^{3+}:\text{GdCl}_3$  with pressure. Solid and dashed lines denote the experimental and calculated data (using the CF parameters in Fig. 3), respectively.



CF parameters is introduced. In the CCF strategy, enormous efforts to reduce the number of CCF parameters and to search for a subset of the parameters particularly effective in dealing with the anomalous multiplets of lanthanide ions have led to the orthogonal CCF,  $\delta$ -function CCF, spin-correlated crystal-field, and orbitally correlated crystal-field (LCCF) models. A more detailed discussion of these models has been given by Reid and Newman.<sup>24</sup>

In addition, an empirical model that considers adjusting the reduced matrix elements of the one-electron CF Hamiltonian with a constant multiplicative factor has been proposed to deal with the anomalous  ${}^2H_{11/2}$  multiplet of  $\text{Nd}^{3+}$  and the  ${}^5D_{1,2}$  multiplets of  $\text{Eu}^{3+}$  in various host compounds.<sup>19,20</sup>

Our present  $\text{Pr}^{3+}:\text{GdCl}_3$  results for the  ${}^1D_2$  CF splittings and their variations with pressure provided the opportunity to gain insight into the CCF effect on the anomalous  ${}^1D_2$  multiplet of  $\text{Pr}^{3+}$ . Let us first take a close look at energy matrix elements of its three CF energy levels in the one-electron CF model:

$$\begin{aligned}
 E(\Gamma_1) &= \frac{2}{5} \sqrt{\frac{2}{3}} B_0^2 \langle f^2 {}^1D || U^{(2)} || f^2 {}^1D \rangle \\
 &\quad + 2 \sqrt{\frac{1}{55}} B_0^4 \langle f^2 {}^1D || U^{(4)} || f^2 {}^1D \rangle, \\
 E(\Gamma_5) &= -\frac{2}{5} \sqrt{\frac{2}{3}} B_0^2 \langle f^2 {}^1D || U^{(2)} || f^2 {}^1D \rangle \\
 &\quad + \frac{1}{3} \sqrt{\frac{1}{55}} B_0^4 \langle f^2 {}^1D || U^{(4)} || f^2 {}^1D \rangle, \\
 E(\Gamma_6) &= \frac{1}{5} \sqrt{\frac{2}{3}} B_0^2 \langle f^2 {}^1D || U^{(2)} || f^2 {}^1D \rangle \\
 &\quad - \frac{4}{3} \sqrt{\frac{1}{55}} B_0^4 \langle f^2 {}^1D || U^{(4)} || f^2 {}^1D \rangle, \quad (2)
 \end{aligned}$$

where  $\langle f^2 {}^1D || U^{(k)} || f^2 {}^1D \rangle$  ( $k=2,4$ ) are the reduced matrix elements. Based on Eq. (2) and using the same empirical model proposed by Faucher and co-workers<sup>19,20</sup> and used in  $\text{Nd}^{3+}$  and  $\text{Eu}^{3+}$ , we can introduce two constant multiplicative factors  $x$  and  $y$  for  $k=2$  and  $k=4$ , respectively, to eliminate the discrepancy in the  ${}^1D_2$  CF splittings for  $\text{Pr}^{3+}:\text{GdCl}_3$  at not only ambient but also high pressure. When a significant admixture of  ${}^1D_2$  with  ${}^3P_2$  ( $0.94|{}^1D_2\rangle + 0.30|{}^3P_2\rangle$ ) via both an intermediate coupling and a CF  $J$  mixing was taken into account, the factors were found for  $x=0.6(2)$  and  $y=1.3(1)$  in the whole pressure range of 60 kbar.

An attempt will be made to find out the physical linkage of the empirical  $x$  and  $y$  factors to the CCF effect. In effect, the  $x$  and  $y$  factors introduced into the  ${}^1D_2$  multiplet are equivalent to including the additional CF operators that reduce the conventional ( $k=2$ ) rank CF contribution by a factor of 0.4 and increase the  $k=4$  rank CF contribution by a factor of 0.3. Yeung and Newman<sup>11</sup> applied the LCCF model to  $\text{Pr}^{3+}:\text{LaCl}_3$  and observed that it is remarkable in this sys-

TABLE II.  ${}^1D$  reduced matrix elements for the LCCF  $V^{(k)}$  and CF  $U^{(k)}$  operators ( $k=2,4$ ) of  $\text{Pr}^{3+}$ . The values for  $\langle ||U^{(k)}|| \rangle$  are taken from Ref. 26.

$\langle   V^{(2)}   \rangle$	$11/70\sqrt{70}$	$\langle   V^{(4)}   \rangle$	$-4/21\sqrt{70}$
$\langle   U^{(2)}   \rangle$	$-11/42\sqrt{6}$	$\langle   U^{(4)}   \rangle$	$2/105\sqrt{55}$

tem and considerably reduces the discrepancy of the anomalous  ${}^1D_2$  multiplet. When the LCCF effect is included in CF calculations, the conventional CF parameters  $B_0^2$  and  $B_0^4$  change from  $106(6) \text{ cm}^{-1}$  and  $-339(13) \text{ cm}^{-1}$  to  $81(14) \text{ cm}^{-1}$  and  $-374(24) \text{ cm}^{-1}$ , respectively, and the other CF parameters ( $k=6$ ) remain nearly unchanged.<sup>11</sup> The absolute value for  $B_0^2$  decreases by a factor of 0.76(16) and increases for  $B_0^4$  by a factor of 1.10(12). Our empirical model used in  $\text{Pr}^{3+}:\text{GdCl}_3$  and the LCCF model considered in  $\text{Pr}^{3+}:\text{LaCl}_3$  show a similar result.

In principle, the LCCF potential can be approximately rewritten by substituting the operators  $C_q^{(k)} + (b_q^k/B_q^k)V_q^{(k)}$  (LCCF) for the one-electron tensor operators  $C_q^{(k)}$  in the conventional one-electron CF potential  $H_{\text{CF}} = \sum_{kq} B_q^k C_q^{(k)}$ , where  $b_q^k$  are the LCCF parameters and were derived,  $b_0^2 = 1.8(1) \text{ cm}^{-1}$  and  $b_0^4 = 4.5(2.3) \text{ cm}^{-1}$ , for  $\text{Pr}^{3+}:\text{LaCl}_3$  (Ref. 11). One can also understand that the contributions of the LCCF  $V_q^{(k)}$  operators result in a change of the conventional CF parameters  $B_q^k$ , a decrease of  $B_0^2$  and an increase of  $|B_0^4|$  for  $\text{Pr}^{3+}:\text{LaCl}_3$ . Furthermore, we evaluated the  ${}^1D$  reduced matrix elements of the LCCF  $V^{(k)}$  operators ( $k=2,4$ ) using formula (11) of Ref. 11. Their values are given together with those of the conventional one-electron CF  $C^{(k)}$  operators in Table II. It is clear from Table II that the LCCF  $V^{(2)}$  operator reduces the contribution of the CF  $C^{(2)}$  operator due to the opposite sign for  $b_0^2 \langle f^2 {}^1D || V^{(2)} || f^2 {}^1D \rangle$  and  $B_0^2 \langle f^2 {}^1D || U^{(2)} || f^2 {}^1D \rangle$ , and the LCCF  $V^{(4)}$  operator increases the contribution of the CF  $C^{(4)}$  operator due to the same sign for  $b_0^4 \langle f^2 {}^1D || V^{(4)} || f^2 {}^1D \rangle$  and  $B_0^4 \langle f^2 {}^1D || U^{(4)} || f^2 {}^1D \rangle$ . We therefore expect that our empirical correction factors  $x$  and  $y$  are physically equivalent to the LCCF effect.

We further note that a  $4f^2-4f^15d^1$  configuration interaction via the odd-rank  $k$  CF terms contributes to the  ${}^1D_2$  CF splittings and eliminates the discrepancy between the experiment and the conventional one-electron CF model description in the case of  $\text{Pr}^{3+}:\text{LaCl}_3$  (Ref. 12). The physical connection between the LCCF effect and this configuration interaction is also clear because the matrix elements of the LCCF  $V^{(k)}$  ( $k=\text{even}$ ) operators are related explicitly to the matrix elements of odd-rank  $U^{(k-1)}$  and  $U^{(k+1)}$  operators.<sup>11</sup>

Burdick and Richardson<sup>13</sup> applied the  $\delta$ -function CCF model in the analyses of ambient pressure  $\text{Pr}^{3+}:\text{GdCl}_3$  and  $\text{Pr}^{3+}:\text{LaCl}_3$  data and obtained an improvement of their fits in the anomalous  ${}^1D_2$  CF splitting simulation by using two additional  $\delta$ -function CCF parameters [ $D_0^2 = -2.8(1.9)$  and  $D_0^4 = 6.0(2.2)$  for  $\text{Pr}^{3+}:\text{GdCl}_3$  and  $D_0^2 = -0.9(1.3)$  and  $D_0^4 = 4.6(1.0)$  for  $\text{Pr}^{3+}:\text{LaCl}_3$ ]. We can also expect that our empirical  $x$  and  $y$  factors are related to their  $D_0^2$  and  $D_0^4$   $\delta$ -function CCF parameters.

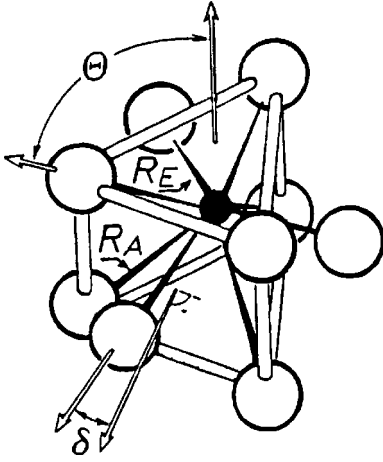


FIG. 5. Coordination polyhedron of  $\text{Cl}^-$  ligand ions around  $\text{Pr}^{3+}$  in  $\text{GdCl}_3$ .

Furthermore, the constant factors  $x=0.6(2)$  and  $y=1.3(1)$  over a wide range of pressure indicate that the CCF effect should have a similar distance dependence as the one-electron CF effect. In contrast, a CCF analysis<sup>15</sup> for the effect of pressure on the energy levels of  $\text{Nd}^{3+}$  in  $\text{LaCl}_3$  showed a strong pressure dependence for the orthogonal CCF  $G_{10A}^4$  parameter. Li and Reid<sup>14</sup> pointed out that the CCF  $g_{10}^K$  operators do not include the LCCF contributions for the  $\text{Pr}^{3+}$  systems discussed by Yeung and Newman,<sup>11</sup> and that the contributions from the CCF  $g_{10A}^4$  and  $g_{10B}^4$  operators to the CF splittings in the  $^1D_2$  multiplet would tend to cancel each other, because their reduced matrix elements for  $^1D_2$  have similar magnitudes and opposite signs. These facts illustrate different CCF effects that influence the  $^2H_{11/2}$  multiplet of  $\text{Nd}^{3+}$  and the  $^1D_2$  multiplet of  $\text{Pr}^{3+}$ .

## V. LOCAL STRUCTURE

$\text{GdCl}_3$  belonging to a class of anhydrous trichlorides has the hexagonal  $\text{UCl}_3$ -type structure (space group  $176-P6_3/m$  or  $C_{6h}^2$ ).<sup>27</sup>  $\text{Gd}^{3+}$  cations position at  $2(d)$  sites:  $(2/3, 1/3, 1/4; 1/3, 2/3, 3/4)$  and  $\text{Cl}^-$  anions at  $6(h)$ :  $(x, y, 1/4; \bar{y}, x + \bar{y}, 1/4; \bar{x} + y, \bar{x}, 1/4)$ . A cation coordination polyhedron consists of nine  $\text{Cl}^-$  anions (Fig. 5), six of which, referred to as apical ligand ions, are located at the upper and lower corners of a tricapped trigonal prism with an interionic distance  $R_A$  from the cation, and three of which, referred to as equatorial ions, are located on the mirror plane at the distance  $R_E$  from the cation. In a spherical coordinate system, the coordinates of these ligand ions are expressed as  $(R_A, \Theta, \Phi)$  for the three upper apical ions,  $(R_A, \pi - \Theta, \Phi)$  for the three lower apical ions with  $\Phi = (2n - 1)\pi/3$  ( $n = 1, 2, 3$ ), and as  $(R_E, \pi/2, \Phi)$  with  $\Phi = \delta + 2(n - 1)\pi/3$  ( $n = 1, 2, 3$ ) for the three equatorial ions.  $\delta$  represents the deviative angle of the equatorial ion relative to the normal of a rectangular face of the trigonal prism (Fig. 5) and has an absolute value less than  $1^\circ$ .

According to the superposition model [Eq. (1)], the total CF contributions from these nine Cl ligands to the CF parameters  $B_0^4$ ,  $B_0^6$ , and  $B_6^6$  of  $\text{Pr}^{3+}$  in  $\text{GdCl}_3$  are given by

$$B_0^4 = \frac{3}{4} \bar{B}_4(R_0) \left[ (35 \cos^4 \Theta - 30 \cos^2 \Theta + 3) \left( \frac{R_0}{R_A} \right)^{t_4} + \frac{3}{2} \left( \frac{R_0}{R_E} \right)^{t_4} \right],$$

$$B_0^6 = \frac{3}{8} \bar{B}_6(R_0) \left[ (231 \cos^6 \Theta - 315 \cos^4 \Theta + 105 \cos^2 \Theta - 5) \times \left( \frac{R_0}{R_A} \right)^{t_6} - \frac{5}{2} \left( \frac{R_0}{R_E} \right)^{t_6} \right],$$

$$B_6^6 = \frac{693}{32\sqrt{231}} \bar{B}_6(R_0) \left[ 2 \sin^6 \Theta \left( \frac{R_0}{R_A} \right)^{t_6} + \cos 6\delta \left( \frac{R_0}{R_E} \right)^{t_6} \right], \quad (3)$$

where the deviative angle  $\delta$  is only involved in  $B_6^6$ . Since  $\delta$  is small,  $\cos 6\delta \sim 1$  and is thus neglected in our following discussion.

In previous high-pressure luminescence studies<sup>7,8</sup> on  $\text{Pr}^{3+}:\text{LaCl}_3$ , the intrinsic CF parameters  $\bar{B}_k(R_0)$  and their distance dependences  $t_k$  of  $\text{Pr}^{3+}-\text{Cl}^-$  ion pairs have been reliably determined for  $\bar{B}_4(R_0) = 235(18) \text{ cm}^{-1}$  and  $\bar{B}_6(R_0) = 267(28) \text{ cm}^{-1}$  with a reference distance of  $R_0 = 295.4 \text{ pm}$ , and  $t_4 = 8(2)$  and  $t_6 = 6(2)$ . When these values are transferred to  $\text{Pr}^{3+}-\text{Cl}^-$  ion pairs in  $\text{Pr}^{3+}:\text{GdCl}_3$ , the local structure around the substitutional  $\text{Pr}^{3+}$  at  $\text{Gd}^{3+}$  sites in  $\text{GdCl}_3$ , characteristic of three local structure parameters  $R_A^l$ ,  $R_E^l$ , and  $\Theta^l$ , can be obtained using Eq. (3) and the observed CF parameters  $B_0^4$ ,  $B_0^6$ , and  $B_6^6$  (Fig. 3).

Our calculated results for the local structure parameters are shown in Fig. 6. The host structure parameters  $R_A^h$ ,  $R_E^h$ , and  $\Theta^h$  (Fig. 5) of  $\text{GdCl}_3$  under pressure were studied experimentally using a high-pressure single-crystal x-ray-diffraction technique<sup>8</sup> and their variations with pressure are also shown in Fig. 6. By comparing the calculated and experimental results, we find similar variations with pressure of the local and host structure parameters with average offsets of  $R_E^l - R_E^h \sim 4.9 \text{ pm}$ ,  $R_A^l - R_A^h \sim 2.6 \text{ pm}$ , and  $\Theta^l - \Theta^h \sim -0.25^\circ$ . The offsets are expected to exist and are attributed to local distortions due to the mismatch in ionic size between  $\text{Pr}^{3+}$  and  $\text{Gd}^{3+}$  ions. The similar variations further indicate that once lanthanide ions are substitutionally incorporated into host lattice crystals, the local surroundings around the central ions distort completely. In other words, one can reasonably assume that local distortions remain constant under pressure.

We can further observe that the two distance distortions are positive and that the distance distortion is larger for the equatorial than the apical bond lengths. The positive distance distortions are due to larger substitutional  $\text{Pr}^{3+}$  ions relative to substituted host  $\text{Gd}^{3+}$  cations in  $\text{GdCl}_3$ . It is experimentally known that the equatorial bond is clearly softer than the apical (see Fig. 2 for the equatorial and apical bond lengths as a function of pressure in  $\text{LaCl}_3$ ,  $\text{PrCl}_3$ , and  $\text{GdCl}_3$ , as well as Fig. 3 for the ratio of the equatorial bond length to the apical ( $R_E/R_A$ ) as a function of the ratio of the lattice

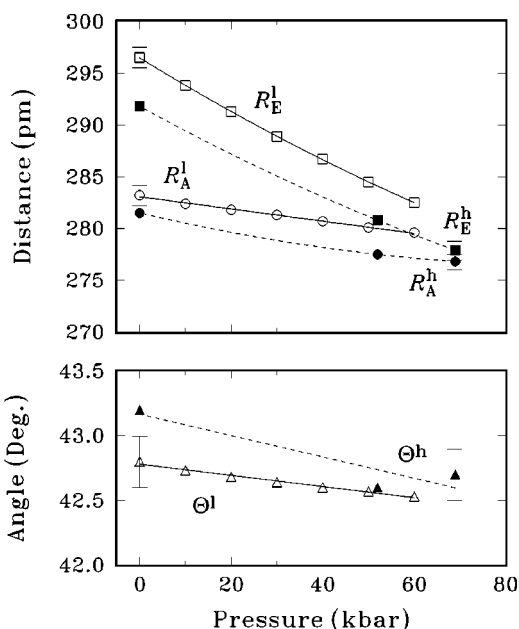


FIG. 6. Variations of the distances and angles of  $\text{Pr}^{3+}:\text{GdCl}_3$  under pressure. Superscripts  $l$  and  $h$  denote the local and host lattice structural parameters. The experimental data for  $R_A^h$ ,  $R_E^h$ , and  $\Theta^h$  are taken from Ref. 8.

parameter  $c$  to  $a$  along a series of anhydrous trichlorides (Ref. 8). Upon substitution of lanthanide ions, the equatorial bond length is expected to distort more easily than the apical. The negative angle distortion is also expected from a systematic decrease in  $\Theta$  over the series of the anhydrous trichlorides of the lanthanides from  $\text{Gd}^{3+}$  to  $\text{La}^{3+}$ .

## VI. CONCLUSION

We have measured luminescence and excitation spectra of  $\text{Pr}^{3+}:\text{GdCl}_3$  up to 60 kbar. The Slater parameters  $F_k$ , spin-orbit coupling parameter  $\zeta_{4f}$ , and crystal-field parameters  $B_0^2$ ,  $B_0^4$ ,  $B_0^6$ ,  $B_6^6$  were determined as a function of pressure.

A large deviation between the calculated and experimental crystal-field splittings of the  $^1D_2$  multiplet for  $\text{Pr}^{3+}$  was observed to exist within a conventional one-electron crystal-field model. We showed that the deviation was primarily due to a neglect of correlation crystal-field effects and that empirical corrections of the reduced matrix elements can be used to more accurately describe the crystal-field splittings in  $^1D_2$ . A detailed discussion of our results indicates that the empirical corrections are physically equivalent to orbitally correlated crystal-field effects.

We also used the superposition model to characterize the local structure of substitutional  $\text{Pr}^{3+}$  ions at  $\text{Gd}^{3+}$  sites in  $\text{GdCl}_3$ . We further found that angular distortions and unequal distortions in the apical and equatorial nearest-neighbor ligand bond lengths are present. More generally, our present results illustrate the potential of crystal-field theory and high-pressure spectroscopy for quantifying the local structure around dopants upon incorporation in host lattices and for developing structure-property relations in optical materials.

## ACKNOWLEDGMENTS

We are thankful to D. Niggemeier for the preparation of the samples used in this study. We would like also to express our thanks to Professor W. B. Holzapfel and Dr. Th. Tröster for the fruitful discussion. This work was supported by the U.S. National Science Foundation under Grant No. DMR-0107802.

- <sup>1</sup>Y. Yeung and D.J. Newman, *J. Phys. C* **21**, 537 (1988).
- <sup>2</sup>J.O. Rubio, C. Ruiz-Mejia, U.V. Oseguera, and H.S. Murrieta, *J. Chem. Phys.* **73**, 53 (1980).
- <sup>3</sup>E.J. Bijvank, H.W. den Hartog, and J. Andriessen, *Phys. Rev. B* **16**, 1008 (1977).
- <sup>4</sup>D. Zevenhuijzen, J.A. van Winsum, and H.W. Hartog, *J. Phys. C* **9**, 3113 (1976).
- <sup>5</sup>M.I. Bradbury and D.J. Newman, *Phys. Chem. Lett.* **1**, 44 (1967).
- <sup>6</sup>D.J. Newman and B. Ng, *Rep. Prog. Phys.* **52**, 699 (1989).
- <sup>7</sup>T. Gregorian, H. d'Amour-Sturm, and W.B. Holzapfel, *Phys. Rev. B* **39**, 12 497 (1989).
- <sup>8</sup>Th. Tröster, T. Gregorian, and W.B. Holzapfel, *Phys. Rev. B* **48**, 2960 (1993).
- <sup>9</sup>Y.R. Shen and W.B. Holzapfel, *Phys. Rev. B* **51**, 15 752 (1995).
- <sup>10</sup>Y.R. Shen and W.B. Holzapfel, *J. Phys.: Condens. Matter* **7**, 6241 (1995).
- <sup>11</sup>Y.Y. Yeung and D.J. Newman, *J. Chem. Phys.* **86**, 6717 (1987).
- <sup>12</sup>D. Garcia and M.D. Faucher, *J. Chem. Phys.* **90**, 5280 (1989).
- <sup>13</sup>G.W. Burdick and F.S. Richardson, *Chem. Phys.* **228**, 81 (1998).
- <sup>14</sup>C.L. Li and M.F. Reid, *Phys. Rev. B* **42**, 1903 (1990).
- <sup>15</sup>C.K. Jayasankar, M.F. Reid, Th. Tröster, and W.B. Holzapfel, *Phys. Rev. B* **48**, 5919 (1993).

- <sup>16</sup>Y.R. Shen and W.B. Holzapfel, *Phys. Rev. B* **51**, 6127 (1995).
- <sup>17</sup>D.J. Newman, *Chem. Phys. Lett.* **6**, 288 (1970).
- <sup>18</sup>B.R. Judd, *Phys. Rev. Lett.* **39**, 242 (1977).
- <sup>19</sup>M.D. Faucher, D. Garcia, and P. Porcher, *C. R. Acad. Sci., Ser. II: Mec., Phys., Chim., Sci. Terre Univers* **308**, 603 (1989). In the case of  $\text{Nd}^{3+}$  ( $4f^3$ ) ions, there are two so-called twin terms  $^2H_{11/2}(1)$  ( $W=[210], U=[11]$ ) and  $^2H_{11/2}(2)$  ( $W=[210], U=[21]$ ), which are coupled to each other within the Coulomb interaction between  $4f$  electrons. Some improvement has been achieved for  $\text{Nd}^{3+}$  in various compounds by multiplying the reduced matrix element  $\langle ^2H(2) || U^{(4)} || ^2H(2) \rangle$  with a constant factor of 1/4.
- <sup>20</sup>O.K. Moune, P. Caro, D. Garcia, and M.D. Faucher, *J. Less-Common Met.* **163**, 287 (1990).  $\text{Eu}^{3+}$  ( $4f^6$ ) ions have three so-called twin terms  $^5D(1)$  ( $W=[210], U=[20]$ ),  $^5D(2)$  ( $W=[111], U=[20]$ ), and  $^5D(3)$  ( $W=[210], U=[21]$ ), which are strongly coupled to each other within the Coulomb interaction between  $4f$  electrons. When the reduced matrix elements  $\langle ^5D(3) || U^{(k)} || ^5D(3) \rangle$  ( $k=2$  and  $4$ ) are adjusted with a same constant 5/3, the large overall CF splitting discrepancies in  $^5D_J$  ( $J=1$  and  $2$ ) of  $\text{Eu}^{3+}$  in 15 different host compounds are considerably eliminated.

- <sup>21</sup>S. Hüfner, *Optical Spectra of Transparent Rare Earth Ion Compounds* (Academic, New York, 1978).
- <sup>22</sup>B.G. Wybourne, *Spectroscopic Properties of Rare Earths* (Wiley, New York, 1965).
- <sup>23</sup>R.S. Rana, J. Shertzer, and F.W. Kaseta, *Lanthanide Actinide Res.* **2**, 295 (1988).
- <sup>24</sup>M.F. Reid and D.J. Newman, in *Crystal Field Handbook*, edited by D.J. Newman and B. Ng (University Press, Cambridge, 2000), Chap. 6, p. 120.
- <sup>25</sup>M.D. Faucher and O.K. Moune, *Phys. Rev. A* **55**, 4150 (1997).
- <sup>26</sup>C.W. Nielson and G.F. Koster, *Spectroscopic Coefficient for the  $p^N$ ,  $d^N$ , and  $f^N$  Configurations* (MIT Press, Cambridge, MA, 1963).
- <sup>27</sup>R.W.G. Wyckoff, *Crystal Structures* (Wiley, New York, 1964), Vol. 2.